Journal of Hazardous Materials 478 (2024) 135516

Contents lists available at ScienceDirect

Journal of Hazardous Materials

journal homepage: www.elsevier.com/locate/jhazmat

Research Article

Comprehensive design and performance validation of a wind tunnel for advanced respirable dust deposition investigations

Ahmed Aboelezz [a], Maria Beltran [b], Michael J. Hargather [a], Mostafa Hassanalian [a,*,1], Pedram Roghanchi [c]

[a] Department of Mechincal Engineering, New Mexico Institute of Mining and Technology, Socorro, NM 87801, USA
[b] Department of Mineral Engineering, New Mexico Institute of Mining and Technology, Socorro, NM 87801, USA
[c] Department of Mining Engineering, University of Kentucky, Lexington, KY 40506–0107, USA

HIGHLIGHTS

- Designed a blowing-type wind tunnel for simulating coal mine dust deposition using ANSYS Fluent.
- Implemented a constant particle delivery system for consistent dispersion.
- Simulated miner inhalation of coal dust using MALDA and custom dust injection.
- Verified airflow and turbulence using dust sensors and a hot-wire anemometer.
- Demonstrated wind tunnel effectiveness in modeling dust deposition for miner safety.

GRAPHICAL ABSTRACT

Design and Performance Validation of Wind Tunnel for Respirable Dust Deposition Studies.
Description: This study presents the design and validation of a wind tunnel to investigate respirable dust deposition relevant to coal mining. Key features include a constant particle delivery system, ANSYS Fluent optimization, and the use of MALDA for realistic dust inhalation simulations.

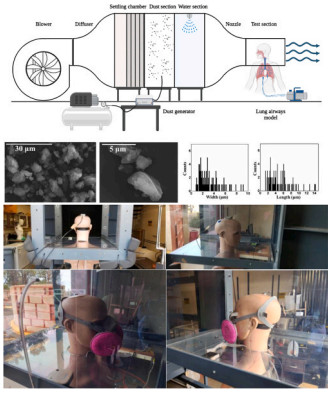

ARTICLE INFO

Keywords:
Computational Fluid Dynamics
Respirable Dust
Wind Tunnel
Mining

ABSTRACT

This study presents the comprehensive design and performance validation of a wind tunnel specifically developed for advanced investigations into respirable dust deposition pertinent to coal mining environments. The design integrates a constant particle delivery system engineered to maintain uniform particle dispersion, which is critical for replicating real-world conditions in coal mines. Our methodology involved using ANSYS Fluent for the design and optimization of a blowing-type wind tunnel, with a focus on controlling turbulence levels and minimizing pressure drops, which are crucial for accurate dust behaviour simulation. The core of our research emphasizes the deployment of the Aerosol Lung Deposition Apparatus (ALDA) alongside a custom dust injection system to measure particle distributions within the test section. This setup enabled us to simulate the inhalation of coal dust particles, providing a realistic scenario for assessing potential hazards to miners. Validation of the

* Corresponding author.
E-mail address: mostafa.hassanalian@nmt.edu (M. Hassanalian).
[1] https://doi.org/10.1016/j.cviu.2017.00.000

https://doi.org/10.1016/j.jhazmat.2024.135516
Received 28 May 2024; Received in revised form 16 July 2024; Accepted 12 August 2024
Available online 13 August 2024

tunnel's performance was achieved through extensive testing with dust sensors and a hot-wire anemometer, which verified the airflow velocity and turbulence against the initial design specifications. The findings affirm the wind tunnel's capability to effectively model dust deposition and its impacts, thereby offering opportunities for enhancing miner safety and health standards.

1. Introduction

Respirable coal mine dust (RCMD) is an inherent byproduct of coal mining activities that raises extraordinary health and safety concerns. Recent findings underscore a significant resurgence of black lung disease among long-tenure coal miners in central Appalachia, USA, with over 20 % of tested miners affected, highlighting persistent failures in disease prevention despite longstanding regulatory efforts [1]. Cumulative inhalation of RCMD can lead to chronic pulmonary diseases including Coal Worker's Pneumoconiosis (CWP), silicosis, mixed dust pneumoconiosis, Dust-related Diffuse Fibrosis (DDF), and progressive massive fibrosis (PMF) [2–6]. Additionally, high concentrations of coal dust create a hazardous atmosphere inside the mines by increasing the risk of explosions, which is one of the most serious hazards in underground mines, which can lead to high mortality rates and great economic loss [7,8]. Therefore, low dust concentrations are required to provide a safe working environment for the coal miners [9].

In [10], researchers evaluated a smart spraying system designed to mitigate airborne PM10 and PM2.5 dusts. Their study included both lab-based tests and field applications in an underground mine to validate the spraying system's efficacy under realistic operational conditions. These experiments were pivotal in examining the interactions between water droplets and dust particles, optimizing the system for enhanced dust suppression in mining environments. However, the integration of a simulated underground coal mine environment, such as the one purposed in the current study, could potentially streamline the evaluation process by consolidating lab and field tests into a single, controlled experiment. Moreover, [11] underscores the utility of specialized environments like dust wind tunnels or consistent particle delivery systems. Their findings demonstrate how such controlled settings can refine dust control strategies by closely replicating real-world conditions, thereby improving health and safety standards in mining operations. [12] further highlights the importance of controlled environments, such as wind tunnels, for the development, testing, and optimization of air curtain dust control technologies. These settings allow for precise manipulation and monitoring of variables that influence dust behavior, which is crucial for effective dust management across various industrial settings. Additionally, [13] discusses the limitations of laboratory experiments in fully capturing the generation mechanisms of coal dust in mines. They advocate for testing environments that more closely mirror actual mine conditions, supporting the relevance of our wind tunnel design as a more representative approach for studying coal dust dynamics.

The utility of dust wind tunnels and consistent particle delivery systems is paramount in advancing our understanding of particle behavior in coal mining environments, where controlling respirable dust is critical for miner safety. Studies such as those by [14] have demonstrated the effectiveness of biopolymers as dust suppressants in wind tunnel experiments, highlighting their potential as environmentally friendly alternatives in mining operations. Similarly, [15] discusses the key design parameters for creating specialized low-density dust wind tunnels that can simulate complex dust dynamics relevant to both terrestrial and Martian environments. Moreover, comparative studies on the transport mechanisms of microplastics and mineral dust by [16] provide crucial insights into particle dynamics, employing wind tunnel methodologies to explore fundamental transport behaviors. This is complemented by [17], who utilized wind tunnel experiments to investigate volcaniclastic dust emissions, further underscoring the importance of controlled experimental setups in understanding particle dispersion under various environmental impacts. Lastly, [18] made study using wind tunnel experiments demonstrated that trees, particularly cypress, significantly reduce PM2.5 concentrations around buildings, enhancing particle removal by approximately 20 % and thereby improving urban air quality.

Having a dust wind tunnel for studying lung dust depositions offers several significant benefits to respiratory health research and occupational safety. First, it allows for the controlled simulation of various environmental conditions, including wind speed, particle size distribution, and humidity, which can affect how dust particles are inhaled and deposited in the lungs. This level of control is critical for understanding the specific conditions that lead to increased risks of respiratory diseases. Second, by replicating real-world scenarios in a controlled setting, researchers can study the efficiency of protective equipment, such as masks and respirators under different conditions, leading to improved design and recommendations for their use. Additionally, the data obtained from these studies can inform regulatory standards for workplace and environmental safety, helping to minimize the risk of lung diseases associated with dust exposure. Lastly, the insights gained from such research can contribute to the development of targeted therapies and preventive measures for those already affected by or at risk of developing dust-related pulmonary conditions, ultimately enhancing public health outcomes.

This study's primary contribution to process safety and risk engineering is through the innovative application of a custom-designed wind tunnel, which provides a controlled environment for the rigorous testing and optimization of dust control measures pertinent to coal mining operations. By simulating realistic underground mine conditions, this research directly addresses critical safety challenges associated with respirable dust exposure, one of the most significant hazards in mining environments. This focus on replicating actual working conditions allows for a detailed analysis of how various dust mitigation strategies, such as the newly tested water spray system and different types of face masks, perform under specific environmental conditions. The outcomes of these experiments provide essential data that can inform safer workplace practices and engineering controls, ultimately leading to reduced health risks and enhanced protection for miners.

In this work, a dust wind tunnel was designed and built to perform several dust-related experiments. Initial sizing of the tunnel was applied using classical wind tunnel design procedures [19]. Using this initial sizing, a design optimization was conducted to reduce the tunnel pressure drop and reduce the turbulence level in the test section. Dust injection mechanisms as well as injection of water droplets were simulated. The manufactured wind tunnel is anticipated to be used along with a 3D-printed innovative Aerosol Lung Deposition Apparatus (ALDA) to investigate respirable dust lung deposition and its adverse effects on the health of mine workers.

2. Wind tunnel design and optimization

The wind tunnel designed here is unique because it allows injection of dust and water droplets into the free-stream flow which then passes into the test section. The design is a non-traditional design with a large settling chamber where the particles are injected, then a nozzle section which accelerates the flow to the test section, as shown in Fig. 1. The wind tunnel design process began with the specifications of the test section, which included a cross-sectional area of 0.25 m^2 and a wind speed range from 0.5 m/s to 3 m/s. The flow velocity range was determined by representative conditions in a mine [20].

The settling chamber is composed of three individual stages: flow conditioning, Dust Injection Section, and Water Injection Section. The alignment of these sections and their interactive dynamics are shown in detail in Fig. 1. The settling chamber sections allow injection, settling, and even distribution of the dust particulates and water droplets. The flow conditioning section includes screens and a honeycomb filter which reduce the turbulence level in the tunnel [21]. The Dust Injection Section was designed to allow for particle injection, where a wide area section with low speeds ensures a good mixture of the dust with the air. In the Water Injection Section ultrasonic and atomizing water spray nozzles are placed to allow investigation of dust control methods [22–24]. The tunnel was equipped with a rail for installation and droplets' injection into the stream along with an optimized drainage system for optimal water removal. The settling chamber, with its screens and honeycomb structure, has an approximate length of 2.37 m.

The settling chamber preceded the wind tunnel's nozzle location directly. The nozzle serves the purpose of increasing the flow stabilization and making the flow region more uniform. The nozzle incorporates a sevenfold reduction ratio, resulting in a cross-sectional area of 3.5 square meters for the settling chamber. Here reference [25] provided valuable insights into the relationship between the length and width of the nozzle. The present design was achieved through application of the computational formulas documented in reference [26], which serve as the foundation of the design process, enabling optimal performance and efficiency. The nozzle was attached to the is the test section, which houses the ALDA. After the test section the flow stream is ejected from the laboratory into the outside atmosphere.

A "push" design was chosen due to the particular characteristics of the particles that will be introduced into the flow stream. By placing the blower at the onset of the wind tunnel, it effectively prevents any dust particles from having an adverse impact on the motor. Moreover, the expulsion of the dust particles from the wind tunnel and the laboratory premises itself serves the purpose of maintaining low concentrations of dust, subsequently safeguarding the researchers who are involved in the experiments. A variable speed blower was selected based on the pressure drop and volumetric flow rate needed through the wind tunnel and to allow continuous variation of the flow velocity.

Due to space constraints on the total length of the wind tunnel, a wide-angle diffuser was incorporated. Drawing on empirical insights from [27], the diffuser is constructed with a 45-degree inclination and an area ratio of 4. Additionally, a single mesh screen is carefully incorporated at the center of the diffuser to ensure optimal flow control. This segment of the design process culminates in a measured length of 1.5 m. Relatively poor flow quality is expected with the wide-angle diffuser, but this is mitigated by the flow control screen section and ultimately by the nozzle into the test section. The mesh size is 1.65 mm, which will inevitably capture some laboratory dust, as is typical with wind tunnel setups. Despite the injection of coal dust occurring post-screen, periodic cleaning of the screens will be conducted to maintain clarity and functionality, as the design of the wind tunnel facilitates easy access to these components.

The optimization of wind tunnel components was important to ensure accurate test results with the desired low tunnel speeds. A critical aspect of the testing process revolves around the nozzle and diffuser, as their shapes have a profound impact on the flow characteristics. ANSYS Fluent software was chosen for conducting in-depth analysis and optimization of these components. The computational fluid dynamics (CFD) analysis, executed via ANSYS Fluent, adhered to the Reynolds-Averaged Navier-Stokes (RANS) equations, pivotal for delineating flow behavior in engineering contexts. The continuity and Navier-Stokes equations are solved finite volume methods to discretize the equations over the computational domain. The incorporation of the $k-\epsilon$ turbulence model enabled the accurate depiction of turbulent kinetic energy and its dissipation, crucial for elucidating complex flow dynamics within the wind tunnel. Precise airflow simulation facilitated the optimization of the tunnel's nozzle and diffuser designs.

Pressure-velocity coupling was implemented using the SIMPLE algorithm, facilitating stability and accuracy by iteratively refining pressure and velocity fields to satisfy continuity constraints. The simulation employed a hexahedral mesh comprising approximately 300,000 elements, balancing computational efficiency with the granularity required for detailed flow analysis.

The initial nozzle geometry, seen in Fig. 2 and depicted by the yellow line, was derived from the original dimensions of the tunnel. By utilizing control points on the curve of the nozzle, as described in [17], its shape was iteratively adjusted by both vertical and horizontal (V and H) control point movement. Each modification subsequently provided valuable information for the computation of airspeed and flow uniformity at the nozzle's exit. The ultimate goal was to achieve a configuration that maximized wind speed while simultaneously maintaining flow uniformity. To achieve this, an exhaustive exploration of various design points was carried out, with wind speed and flow uniformity parameters being recorded as shown in Figs. 2b and 2c. These results were analyzed using a response surface methodology, which involved mapping the variations of design points against wind speed and flow uniformity then employing a min-max search on the response surface. As shown in the response surface results there are two surfaces, one presents the relation between V, H, and the air flow uniformity (U), While the other one is the relation between V, H, and the air flow speed (Vo), based on the color maps chosen, the red values are the highest values. Unfortunately, it is impossible to obtain a design point which could simultaneously provide the highest values for the flow uniformity and the airspeed. However, the design point shown in the figure was chosen to obtain a compromise value between these two. The optimization of the nozzle design resulted in a velocity increase from 3.4 m/s to 3.5 m/s, an improvement of approximately 1.8 %. In contrast, flow uniformity

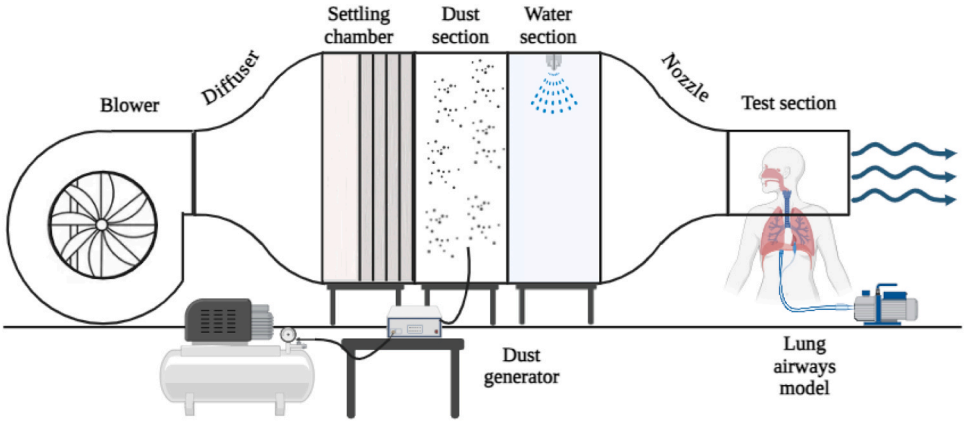

Fig. 1. Schematic representation delineating core components of the wind tunnel.

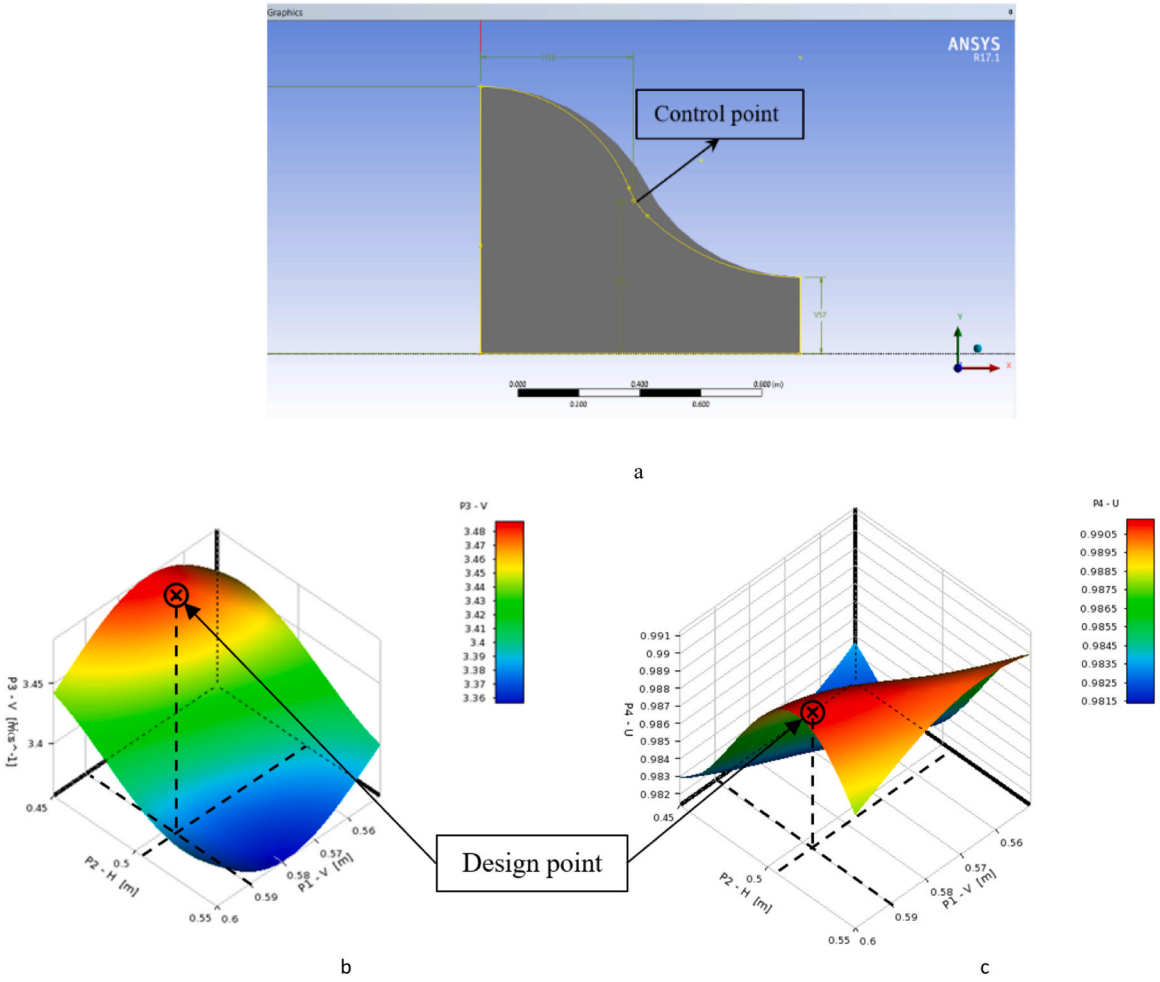

Fig. 2. Design optimization of the tunnel nozzle. a. Optimization of the nozzle shape using ANSYS fluently. b Results of the shape optimization study for wind speed design parameter. c Results of the shape optimization study for uniformity design parameter.

slightly decreased by −0.448 %, changing from 0.986 to 0.981.

Following the optimization process, the finalized shape of the nozzle, denoted by the gray contour in Fig. 2a, was modeled using ANSYS Fluent. This allowed for the visualization of salient flow features such as velocity vectors and pressure contours, as depicted in Figs. 3a and 3b, respectively. The design of the wind tunnel utilized ANSYS Fluent's Discrete Phase Model (DPM) to precisely simulate the dust injection process. This model is adept at capturing the interactions between discrete particles and a continuous fluid phase, ideal for monitoring particle trajectories and behavior in airflow. Dust particles, introduced at the nozzle entrance with specified properties (density of 2400 kg/m^3 and diameter of 0.0006 m), were thoroughly tracked to assess dispersion uniformity and integration effectiveness. These parameters were chosen to simulate extreme conditions within the wind tunnel, ensuring the

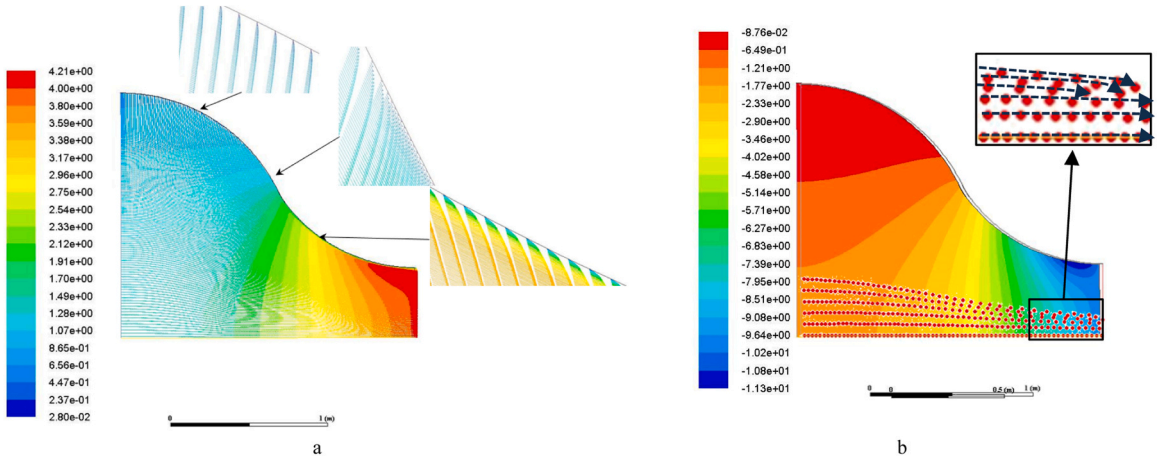

Fig. 3. Results from the CFD analysis. a Velocity streamlines of the optimized nozzle shape. b Pressure contours of the optimized nozzle shape with Path lines of injected dust.

system's robustness by testing with larger and heavier particles than typically encountered. This approach validates the wind tunnel's performance across a broader range of potential real-world scenarios, guaranteeing its effectiveness with various dust particle sizes and densities. These simulation results are depicted in Fig. 3b, effectively illustrating the uniform distribution and successful integration of dust particles within the tunnel's airflow.

3. Fabrication of the dust tunnel

The wind tunnel's structure was constructed using 6 mm thick steel. The nozzle and diffuser pieces were fabricated using a laser cutting process, then welded to the frame. An additional layer of a 2 mm thick sheet metal was then applied to sheath the interior of the nozzle and diffuser. This addition not only contributed to the structural rigidity but also enhanced the streamlined flow dynamics within these specific sections. To optimize visibility, the settling chamber and test sections of the wind tunnel were made from a 10 mm thick acrylic sheet. The final wind tunnel post manufacturing is shown in Fig. 4. The various sections of the wind tunnel were interconnected using external bolts and nuts, enhancing structural integrity. To ensure airtight sealing at the intersections between sections, silicone sealant was applied.

4. Characterization of the coal sample

Representative Pennsylvania Coal dust was injected into the tunnel. The coal used was characterized in terms of the size, shape, and mineral composition of the particulate. A scanning electron microscope from the Center of Integrated Nanotechnologies (CINT) was used to measure the particle size distribution. The results showed that the majority of the coal dust particles displayed smaller sizes than 10 μm (supra-micron), and only 7 % of the particles within the sample had sizes of over 10 μm [27]. Fig. 5 shows scanning electron microscopy (SEM) images of the samples as well as the counts for length and width dimensions in μm. The mean width and length of the particles and the size fractions are shown in Table 1.

4.1. Minerals in the sample

To determine the prevalent minerals present in the sample an X-ray diffraction (XRD) analysis was carried out. Fig. 6 shows the overall XRD spectrum, and the peak list generated by the primary components. The results obtained from the sample corresponding to Pennsylvania coal present three main peaks, that correspond to the main mineral components as well as significant deviations which modify the reference for measuring each peak. These deviations indicate the presence of significant content of amorphous material, which corresponds to organic matter. Coal is characterized for having organic matter randomly distributed along with two components: minerals and macerals. During comminution processes, the resulting particles may contain variable proportions of the three components. In consequence, coal is a remarkably heterogeneous material, posing challenges in terms of characterization [28].

The abundance of the compounding minerals was estimated by choosing the highest individual peak for each one. The highest peak was found in the position $2\theta \sim 26.65^{\circ}$, which corresponds to quartz. The following peak was located at $2\theta \sim 12.38^{\circ}$ angle that corresponds to kaolinite. The last representative peak is indicative of pyrite. Finally the sample presented traces of possibly Illite, which is a secondary mineral as a result of the weathering of muscovite, and displays the same crystalline structure [29,30]. Muscovite is mainly present in metamorphic and acid igneous rocks [31], which makes it improbable for this mica to be present in the sample, since coal is of sedimentary genesis.

4.2. Elements in the sample

A total digestion process was carried out to identify the elements in the sample. In this case, the equipment used was equipped with a high-performance microwave system (model ETHOS UP). The concentration of the elements in the sample was determined and both results were compared to identify the elements most likely present in the sample [27] as reported in Table 2.

From Figure it can be observed that the element that presented the highest concentration in the sample was silicon, which is congruent with the results obtained by the XRD in which quartz (SiO_2) was identified as the mineral with the highest prevalence. The other two major components are also aligned with the XRD result due to the fact that kaolinite is a hydrated aluminosilicate ($Al_2Si_2O_5(OH)_4$) and pyrite is an iron sulfide (FeS_2). From the trace element information, titanium has a comparatively higher concentration than the other elements which exhibited concentrations below 60 μg/g [27].

Numerous coal characterization studies have identified titanium as a common trace element in coal samples. In a significant 1975 campaign, the United States Geological Survey (USGS) analyzed 799 coal samples from various deposits across the country. Specifically, over 90 anthracite samples from the Pennsylvania coal region were examined, all of which contained titanium [32]. These findings revealed that titanium constituted 0.15 % of the anthracite samples, surpassed only by more abundant elements such as Fe, K, Na, Mg, Ca, Al, and Si, which collectively represent a greater proportion of the earth's crust at 0.57 % [32]. Further USGS research indicated that the average titanium content in U. S. coal deposits is approximately 0.08 %. This research also highlighted that titanium is linked to both organic and inorganic processes, contributing to its widespread presence in coal formations [33].

Recent characterization studies have identified titanium, in the form of TiO2, as a significant component in the ashes of several coal samples

a b c

Fig. 4. Wind tunnel manufacturing. a Detailed scheme of the wind tunnel. b The wind tunnel settling chamber. c Wind tunnel nozzle and test section.

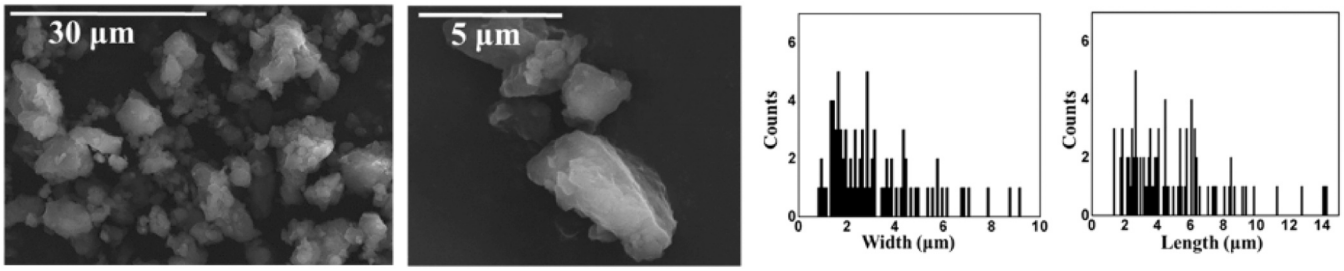

Fig. 5. SEM Results from Pennsylvanian Coal Sample [13].

Table 1
Mean width and length for Pennsylvania coal sample [13].

Coal sample	Mean Width (µm)	Mean Length (µm)	PM1.0 %	PM2.5 %	PM4.0 %	PM10 %
Pennsylvania	3.24 ± 2.00	5.07 ± 3.10	4	44	73	99

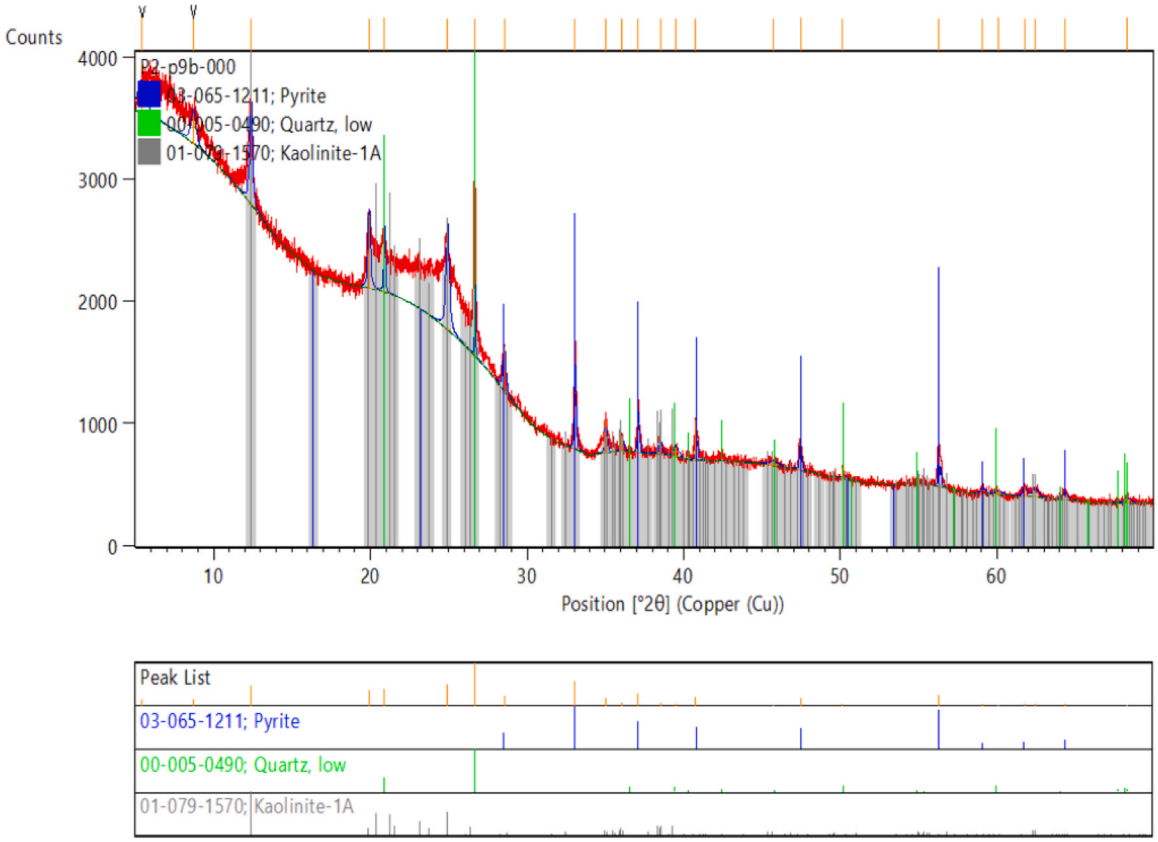

Fig. 6. XRD Results-Pennsylvania Coal.

from Pennsylvania mines, with concentrations ranging between 1.5 % and 3 % [34].

Titanium is recognized for its bio-inert properties and is extensively used in medical and dental applications. Generally, this element poses minimal health risks. However, with the increased use of titanium for biological purposes, there has been a growing interest in conducting more comprehensive studies on its effects. In the field of dentistry, certain studies indicate that corrosion from titanium-alloy dental parts may release particles that lead to bone loss, infections, and conditions such as yellow nail syndrome [35]. Animal tests have demonstrated that when ingested, titanium can cross the intestinal barrier, enter the bloodstream, and potentially cause stomach inflammation, liver necrosis, and cardiovascular lesions. Furthermore, TiO2 has been classified as a Type 2B carcinogen by the International Agency for Research on Cancer (IARC), suggesting it is possibly carcinogenic to humans and highlighting the need for further research to clarify its safety levels [35]. Despite ongoing studies, the full scope of titanium's toxicity in humans remains under-explored.

4.3. *Specific surface area and micro-pore composition*

The surface area of the sample was determined using a seven-point Ns absorption isotherm. For this sample, it was found a specific area of 7.11 ± 0.23 m^2/g. Later the micro-pore analysis showed the sample to be mesoporous, which is a material with a large and uniform pore structure. The pores are characterized for having diameters within

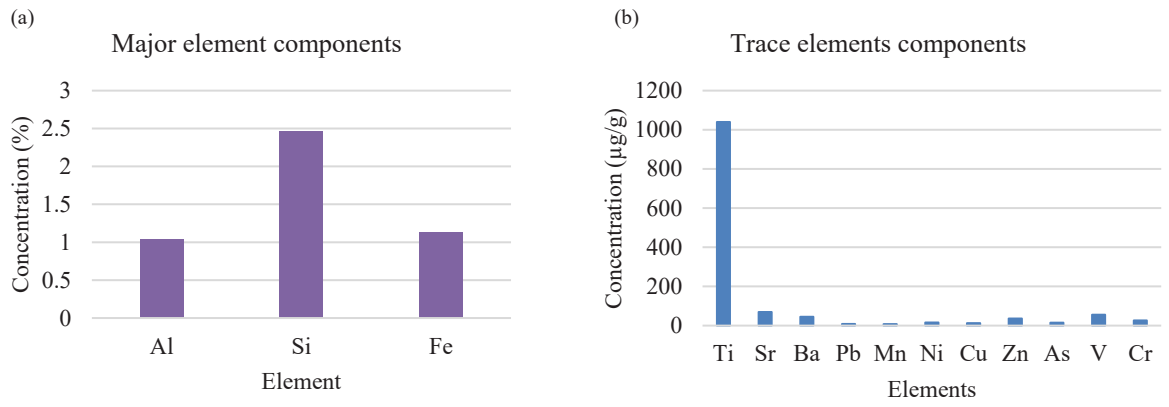

Fig. 7. (a) Major components in the Pennsylvania coal sample. (b) Trace elements components in the Pennsylvania coal sample [26].

Table 2
Elements present in Pennsylvania coal sample.

Sample	Al %	Si %	Fe %	Ti µg/g	Sr µg/g	Ba µg/g	Pb µg/g	Mn µg/g	Ni µg/g	Cu µg/g	Zn µg/g	As µg/g	V µg/g	Cr µg/g
Pennsylvania coal	1.03	2.46	1.13	1040	69.2	45.0	8.7	8.0	16.0	13.0	36.3	14.8	55.4	26.1

0.2–2.0 nm[36,37]. The half-size pore distribution was determined to be 58.81 Å [36].

4.4. Comparative analysis of laboratory and mine-generated Dust

In a previous study, bulk samples from coal seams at mining faces were collected alongside dust samples to perform a comparative analysis. This was intended to closely represent the material converted to dust during mining activities. Analysis confirmed that the lab-generated dust shared similar characteristics with mine-generated dust, particularly in terms of particle size distribution and shape. The particles were predominantly irregular in shape, with sizes ranging from 1.55 to 3.8 µm. Over 60 % of these particles were PM4, falling within the respirable range, and the entirety was classified as PM10 [38].

X-ray diffraction (XRD) analysis of these samples identified primary components including quartz, kaolinite, and smaller quantities of pyrite, muscovite, and calcite—comparable to those used in this experiment [38].

Additional characterization of coal dust samples was conducted in 2019, involving 79 samples from four underground mines across different coal regions in the U.S. These samples, collected using an escort EFL pump equipped with a 10-mm nylon Dorr-Oliver cyclone, also predominantly comprised respirable particles (PM10), aligning with our experimental samples. Chemical analyses of these samples confirmed major elements such as Si, Mg, Al, K, Fe, and Zn, with trace elements including Cu, Ba, Co, Ni, Mn, Cr, and Ag, demonstrating a correlation with the major elements found in our study's samples. Notably, some elemental variations reflect the distinct geological characteristics of the coal deposits [39].

5. Wind tunnel airflow analysis

Hot-wire anemometry was used to measure the velocity and velocity fluctuations throughout the wind tunnel test section. It was essential to accurately determine both the speed of airflow and the turbulence, as these factors greatly affect how coal dust is distributed and concentrated, ultimately impacting where the particles end up in the respiratory systems of workers. To ensure the reliability and accuracy of the hot-wire measurements, a careful calibration procedure was carried out. This involved designing and implementing a calibration setup that precisely aligned the hot-wire probe with the flow of air. To calibrate the hot-wire anemometer to the desired standards, a pitot tube was used as a reference. Fig. 8a and b exhibit the arrangement utilized for the implementation of hot-wire anemometry within the dust wind tunnel, which is made possible by the presence of a traversing system. The traversing system allows for precise placement of the hot-wire probe in different sections of the wind tunnel, namely the inlet section (i), the middle section (m), and the outlet section (e).

The boundary layer was also measured using a grid consisting of 14 points, with each point being 1 mm apart from the others. This careful arrangement allows analysis of the airflow in close proximity to the tunnel walls.

Moreover, Fig. 8c and d provide an outline of the freestream characterization which was measured at points positioned at a fixed distance of 10 cm from each other across the tunnel cross-sectional area.

The depicted results of the boundary layer in Fig. 9 show that the boundary layer is less than about 2 mm in heights across the inlet, middle, and outlet sections. The overall trend and pattern of wind speed remains largely and predominantly consistent. This consistency may be attributed predominantly to the stability and steadiness of the airflow within the tunnel. Furthermore, the consistent profiles of the boundary layer that are observed across the inlet, middle, and outlet sections strongly and convincingly suggest and indicate that the design and structure of the tunnel effectively and efficiently manages the development and progression of the flow from the beginning to the end.

The contour plots in Fig. 10 representing various frequencies shows a detailed visualization of the average wind speed and turbulence levels within the distinct sections of the wind tunnel. The depiction of wind speed manifests through a color gradient, showing the intensity and spatial distribution of airflow throughout the different segments, namely the inlet (i), the middle (m), and the outlet (e), for the frequencies of 10 Hz, 20 Hz, 30 Hz, and 40 Hz.

The analysis of these plots reveals several noticeable observations of significant importance. First and foremost, the contours showing wind speed demonstrate a varied and diverse distribution across the sections, with higher speeds mainly concentrated in the central regions. This interesting phenomenon suggests the presence of a well-organized and consistent airflow within the tunnel's core.

When looking at the contours illustrating turbulence levels, a fairly consistent pattern is visible. Localized areas of heightened turbulence can be attributed to the interaction between the airflow and the tunnel's structural components.

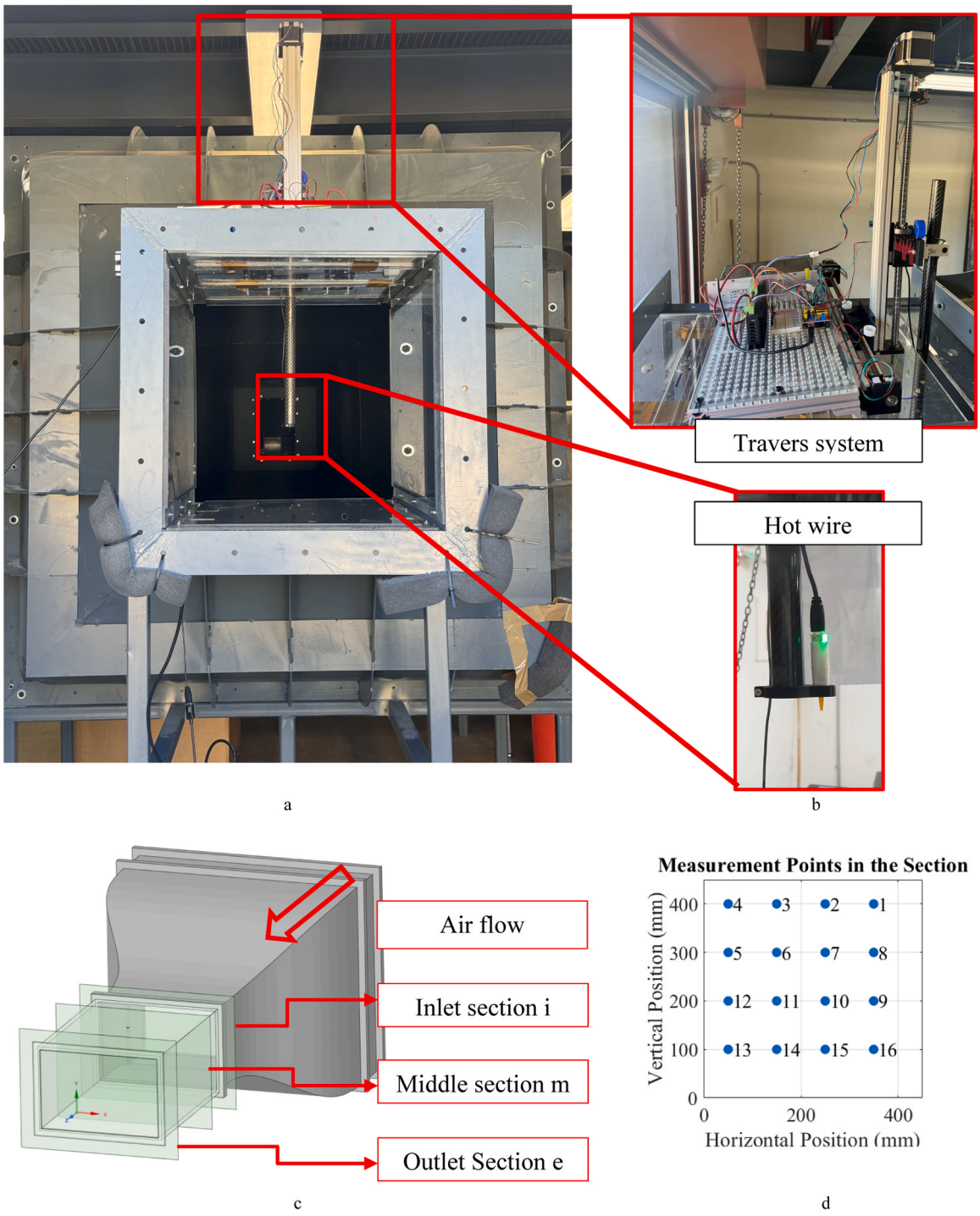

Fig. 8. Installation of Hot-Wire Anemometer in Dust Wind Tunnel. The image displays the traversing system used for the precise positioning of the hot-wire probe across inlet, middle, and outlet sections of the tunnel, with a detailed schematic of the measurement points for airflow and boundary layer analysis at 1 mm and 10 cm intervals, respectively.

Furthermore, an interesting trend emerges when examining the impact of higher frequencies on average wind speed and turbulence levels. It becomes clear that both variables experience a slight increase as the frequency rises. This intriguing phenomenon can be traced back to the greater sensitivity of the measurement equipment used at these higher frequencies. As a result, the equipment can capture a wider range of fluctuations in wind speed and turbulence, including the smaller details that may have gone unnoticed before. Usually, the underground coal mines will have flow fluctuation and relatively high turbulence level. However, the current wind tunnel offers similar conditions which purpose a good fit tool in simulating these mines.

Table 3 provides a summary of the results depicted in Fig. 10. The data shows that the maximum average airspeed recorded is 3.2 m/s, with turbulence levels ranging from 8 % to 11 %.

6. Dust injection experimental setup and procedure

An aerosol generator from Topas (SAG 410/U) was used to inject dust as shown in Fig. 11a. The aerosol generator allows it to work within a wide range of dust concentrations. For analyzing the distribution of the

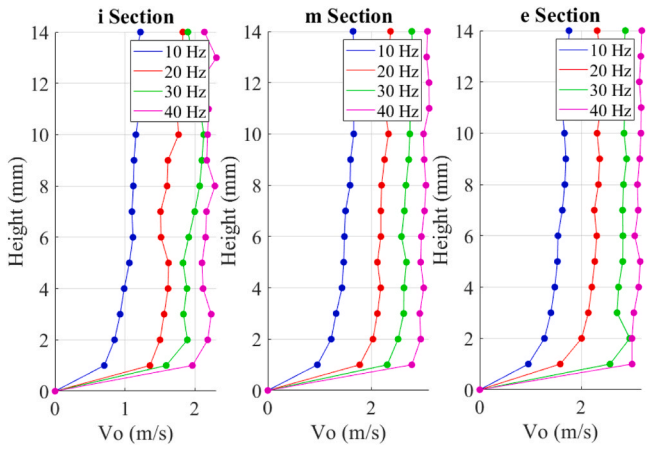

Fig. 9. Boundary Layer Velocity Profiles in Wind Tunnel Sections. The graph delineates the wind speed profiles at varying heights within the inlet, middle, and outlet sections of the wind tunnel, captured at 10, 20, 30, and 40 Hz frequencies, underscoring the stability and consistency of the boundary layer across the tunnel's length, essential for accurate dust dispersion analysis.

dust concentrations inside the tunnel test section, several blower frequencies from 10 Hz to 40 Hz with a step 10 Hz and aerosol injection rates between 10 % to 50 % with step of 10 % from the overall injection rate were tested.

To measure the dust concentration in the test section, four dust sensors were installed as shown in Fig. 11 b and c. SENSIRION SPS30 was used as it can measure dust with a range of 0.3 micrometer to 10 micrometers. The dust sensors were placed in two configurations. In the initial configuration, the sensors were placed at the four corners of the test section. This configuration enables a comprehensive analysis of the spatial distribution of the dust concentration across the entirety of the cross-section of the wind tunnel. In the subsequent configuration, the sensors were placed in a linear fashion, directly coinciding with the direction of the flow. This linear arrangement was used to gauge the longitudinal variations in dust concentrations. The significance of this arrangement lies in its ability to effectively assess the uniformity of dust distribution along the flow direction.

Placing the sensors at the corners can reveal the presence of vortices or secondary flows that may impact the concentration of dust. On the other hand, the linear arrangement can give information about the primary flow characteristics and how they affect the movement of dust. This approach of using two configurations was found to be good to study the complex dynamics of particulate matter in the controlled aerodynamic environment.

During each experiment, the blower was turned on first, followed by the aerosol generator, to create uniform dust concentration inside the settling chamber and minimize any deviations in the results. The equipment was allowed to run for 5 min before taking measurements with the sensors. Once the sensors started recording, each experiment lasted for 20 min and was repeated at least twice. During this time, the 4 sensors provided measurements every second in $\mu g/m^3$. After each experiment, the outlet and the hose connected to the tunnel were thoroughly cleaned to remove any dust buildup.

Fig. 11 d shows the interaction of the dust sensor with air with the help of flow visualization using laser and smoke. Based on the BL measurements in the pervious section and the BL shown in the figure, the dust sensor high is larger than the BL (about 2 mm), which shows how the sensor is measuring the dust in the free stream. The measuring location of the sensor should not be pointed to the behind the sensor as there is the separation vortex as shown in the figure. Also, it is good to locate the measuring point at the start location of the sensor, so the measurement is not affected by the BL on the sensor surface itself. Placing the sensors behind each other should consider at least 5 times the sensor length to avoid the interference in dust measurement due to afterbody vortex.

6.1. Results and discussion of dust experiments

The primary findings were summarized in a series of time history results and bar graphs. First the dust time history for the inline sensors arrangement is shown, the results show the sensitive response of the dust concentration level inside the wind tunnel as a function of changing the dust injection rate. The bar graph distilled the averaged readings from all four sensors in the corner's arrangement. These visuals gave a clear comparison of dust mass concentrations in various operational settings. To gain a deeper understanding, our analysis was expanded to provide specific average mass concentration values for each sensor. This exercise illuminated nuances like particle dispersion uniformity and pinpointed potential concentration gradients or aberrations within the test section. The first set of results in Fig. 12 presents the bar charts of the average of the four sensors dust mass concentration for different dust generator injection rate (aerosol generator), each figure is for a different wind tunnel motor operation Hz.

The outcomes of this validation experiments underscore several noticeable insights into the wind tunnel's performance and operational characteristics:

1. *Particle Distribution and Tunnel Effectiveness:* One of the observations is the uniform distribution of dust particles within the test section.
2. *Correlation Between Dust Injection and Particle Mass Concentration:* As anticipated, a discernible relationship was evident between the volume of injected dust and the resultant particle mass concentration in the test section. As dust injection quantities increased, there was a proportional rise in particle mass concentration. Such a trend accentuates the sensitivity and adaptability of our apparatus to changes in operational parameters.

However, amidst these positive outcomes, there are specific nuances and anomalies that warrant deeper scrutiny:

1. *Non-Linearity in Aerosol Generator Injection:* The injection dynamics of the aerosol generator revealed a non-linear characteristic. This suggests potential fluctuations or inconsistencies in the generator's output across its operational spectrum. Such non-uniform behavior could inadvertently affect concentration gradients within the wind tunnel. Future experimental designs and result interpretations should duly account for this factor.
2. *Anomaly in S3 Sensor Readings:* Throughout our experiments, the S3 sensor consistently presented anomalous readings, showcasing an offset. To determine the root cause, we interchanged its position with the S2 sensor. The deviation remained unchanged, thereby ruling out its location within the tunnel as a contributing factor. Instead, the anomaly appears to be intrinsic to the S3 sensor. To ensure the integrity of future data collection, it might be imperative to recalibrate or replace this sensor.

These observations, both affirmative and critical, provide a roadmap for further enhancements, calibrations, and adaptations in our wind tunnel setup and experimental framework.

6.2. ALDA dust experiments

The Aerosol Lung Deposition Apparatus (ALDA) experiments inspired from [40] represent a cornerstone of the current investigation, designed to bridge the gap between theoretical models and real-world respiratory dynamics in dusty environments. By simulating human respiration within a controlled wind tunnel setting, these experiments provide invaluable insights into the behavior and deposition of aerosolized particles during inhalation. This section details the experimental

setup that replicates the upper respiratory tract of humans, incorporating a throat-like structure to enhance the realism of the simulations. Through these experiments, it was amid to quantify the size and distribution of particles that penetrate deep into the lungs, thereby assessing the associated health risks. This comprehensive approach allows for a more accurate evaluation of dust exposure impacts in occupational settings, particularly in the mining industry.

The experiment depicted in Fig. 13 aims to simulate the process of human inhalation within the confines of the wind tunnel environment, specifically for the purpose of evaluating the inhalation of aerosolized particles. The model, which imitates the upper respiratory tract found in humans, has undergone modifications in order to incorporate a structure that resembles a throat omitting the complex structure of the nasal cavity to specifically focus on assessing dust distribution within the ALDA. This particular alteration plays a vital role in establishing a pathway that is more akin to reality, allowing for the measurement and analysis of particles that are inhaled.

Attached to this model is a device designed to measure the size of

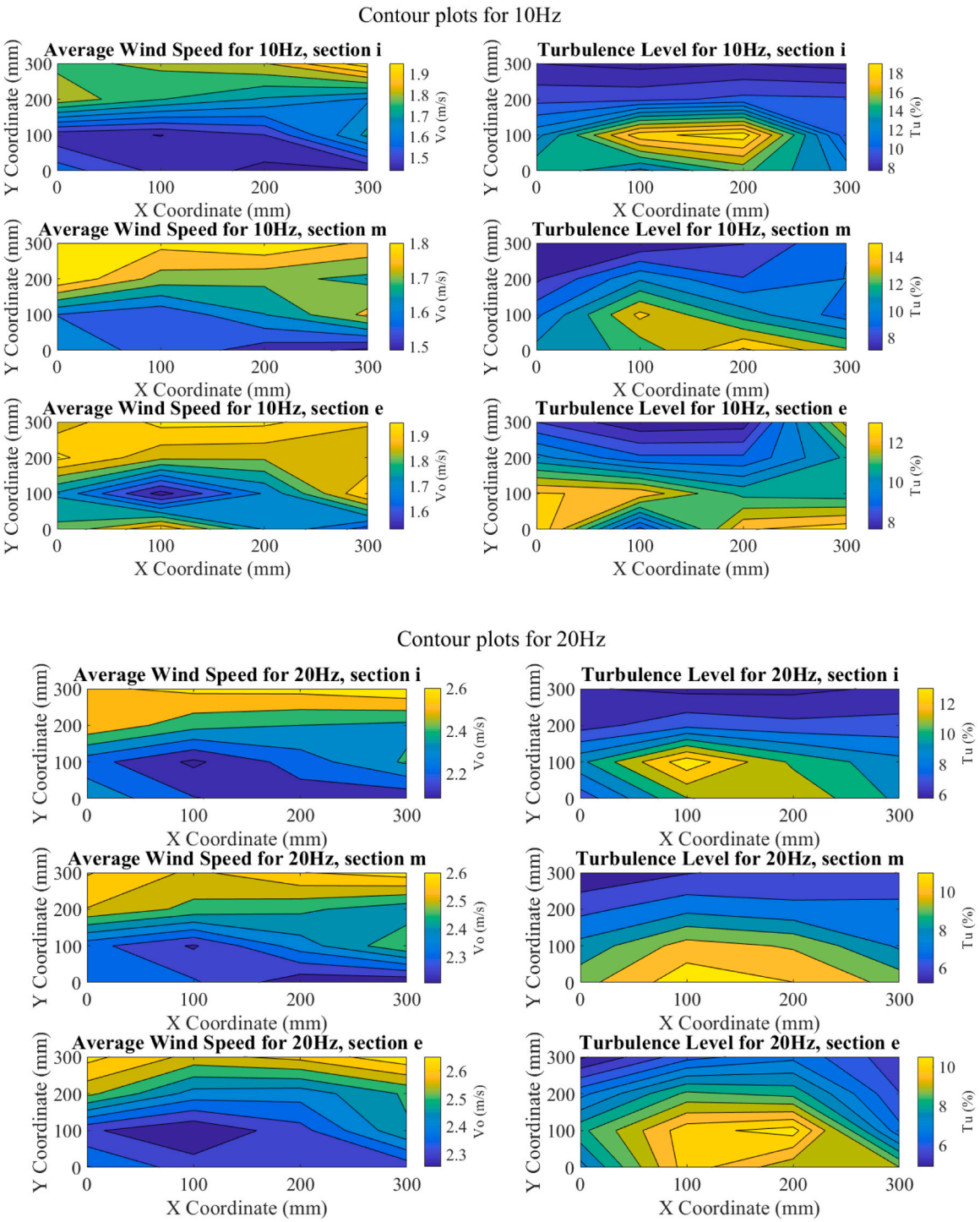

Fig. 10. Contour Plots of Wind Speed and Turbulence Levels. The series of contour plots illustrates the distribution of average wind speed and turbulence levels across inlet, middle, and outlet sections of a wind tunnel at 10 Hz, 20 Hz, 30 Hz, and 40 Hz frequencies, providing a multi-faceted view of the aerodynamic conditions for each section, vital for the assessment of dust dispersion and aerodynamic studies.

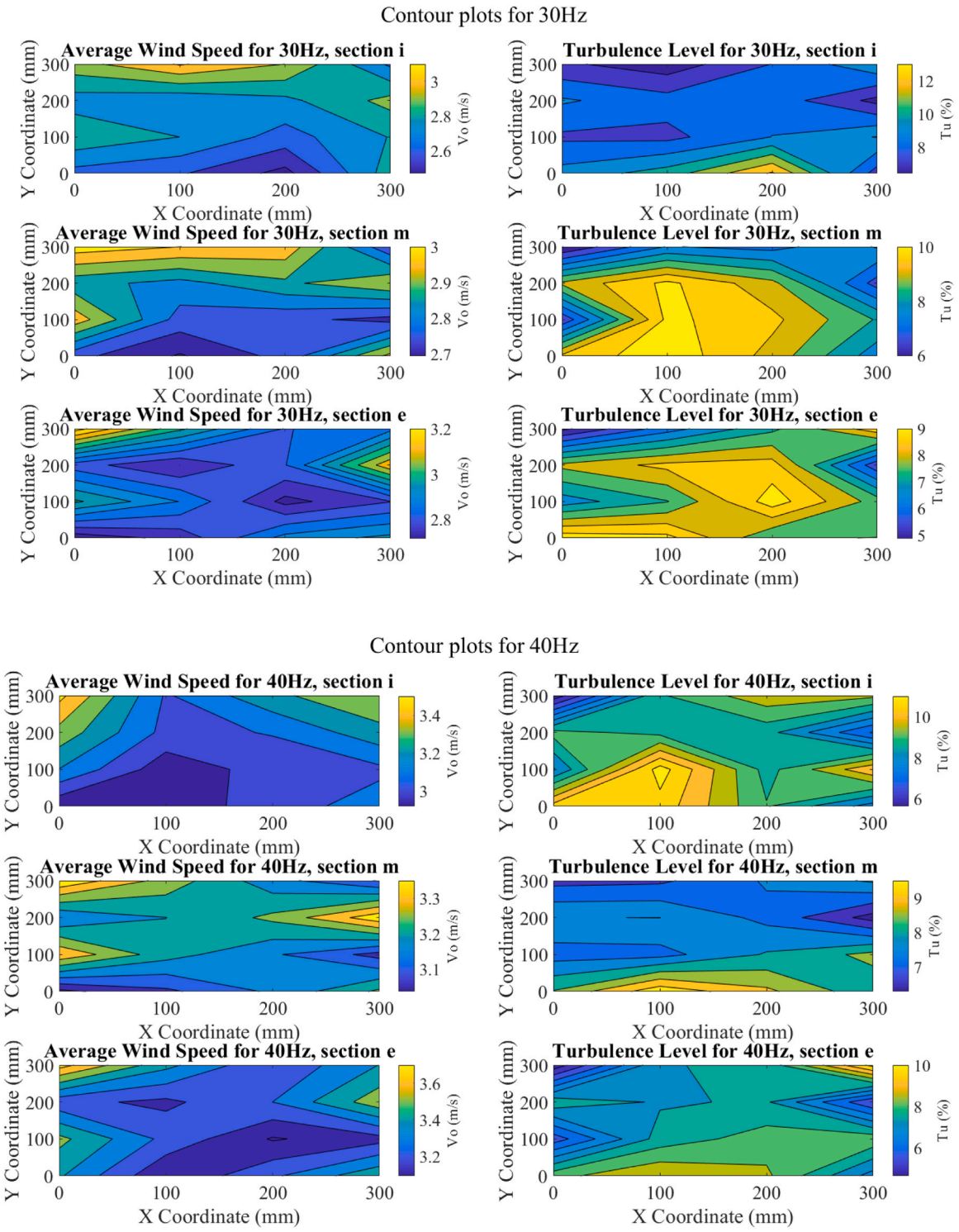

Fig. 10. (*continued*).

Table 3
Average Vo and Average Tu in all sections.

Hz Parameter	10	20	30	40
Average Vo m/s	1.723	2.416	2.850	3.233
Average Tu %	10.90	8.17	8.30	8.16

aerosol particles. This device is to be used to determine the range of particle sizes inhaled. It is important because smaller particles can go deeper into the lungs and pose a greater health risk.

The picture also shows a vacuum pump suction line, which is an essential part of this experiment. The pump creates negative pressure to simulate inhalation, drawing air and dust particles into the model's throat structure. This process mimics the way humans breathe in a dusty environment, allowing researchers to study the quantity and characteristics of particles that enter the respiratory tract.

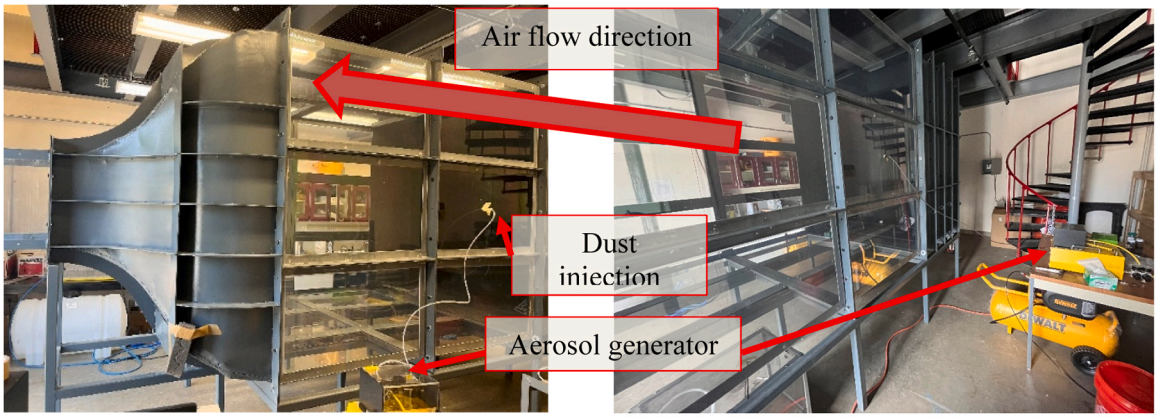

a

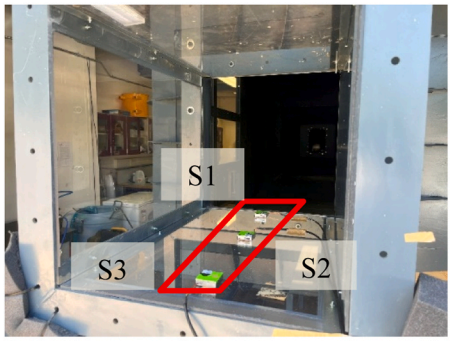

b

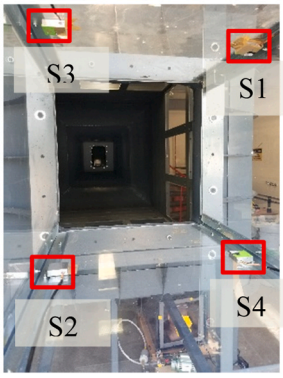

c

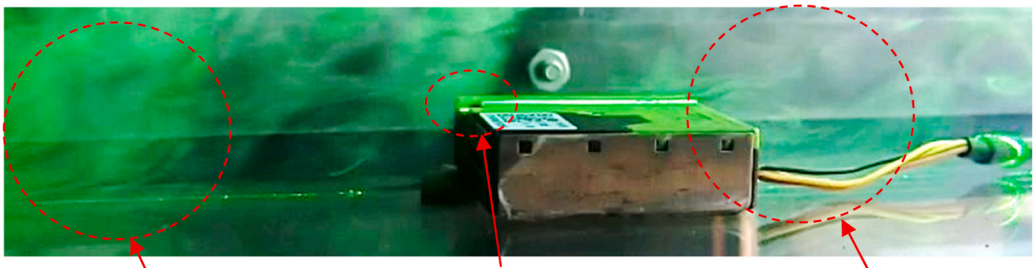

d

Fig. 11. Performance Validation Instruments: A comprehensive view of the integrated aerosol generator at the dust injection section, the strategically placed dust sensors in both linear and circumferential configurations.

The hot wire anemometer's placement is crucial for measuring the speed of the air as it enters the model. Accurately measuring airflow velocity is essential for simulating the conditions of human respiration, including the rate and pattern of airflow.

The results in Fig. 14 show the association between the flow rate of the pump and two pivotal parameters: the speed of airflow within the model and the concentration of dust inside the model. This experiment was carried out in a wind tunnel under a fixed frequency of 20 Hz and a dust injection rate of 20 %.

Fig. 14 a show the relationship between the speed of airflow and the "inhalation" pump flow rate. The graph reveals a positive correlation between these two variables. As the flow rate of the pump increases, the airspeed within the model also increases. This demonstrates that the system responds in a predictable manner to variations in the pump flow rate. This relationship is of great importance when it comes to simulating inhalation since the flow rate must replicate the different speeds at which humans breathe under varying levels of exertion.

Fig. 14 b, on the other hand, showcases the connection between the concentration of dust and the pump flow rate. Interestingly, the dust concentration reaches its peak at a specific flow rate and subsequently decreases as the flow rate continues to increase. There are several possible explanations for this phenomenon. It is possible that the

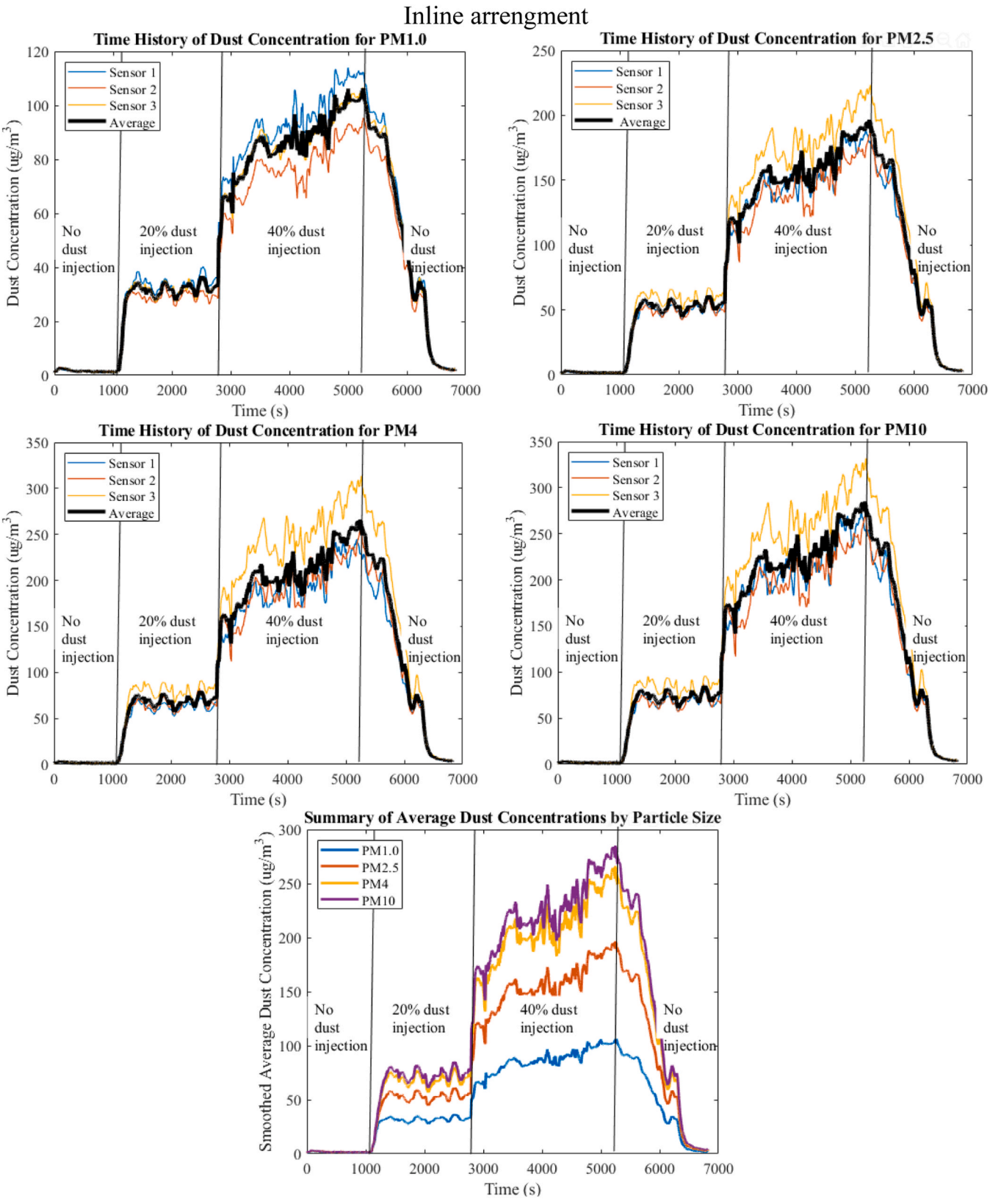

Fig. 12. Bar Graphs of Dust Mass Concentration: Comparative analysis of dust mass concentrations under wind tunnel frequencies of 10, 20, and 30 Hz, with the aerosol generator operating between 10 % to 50 % of its maximum capacity.

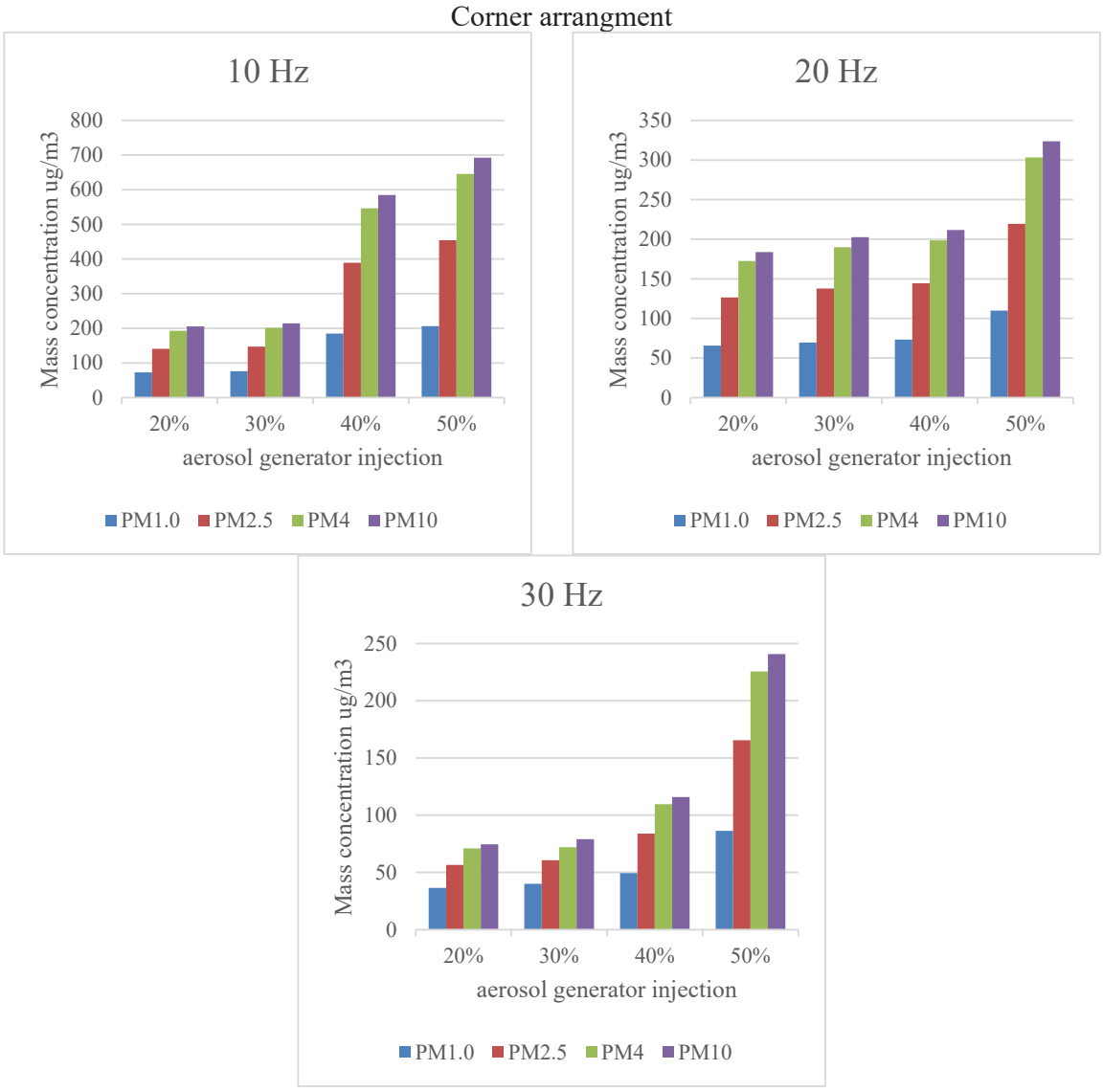

Fig. 12. (*continued*).

increased airflow aids in the dispersion and dilution of particles, resulting in a decrease in their concentration. Alternatively, there may be more intricate interactions between the flow dynamics and the behavior of particles within the model that contribute to this pattern.

Fig. 14 c provides a visual representation of the history of dust concentration throughout the duration of the experiment in the wind tunnel using the external dust sensors. While there are fluctuations in the concentration of dust over time, it generally remains within a certain range. This suggests that there is a relatively stable dispersion of particles over time. The different lines in the graph, corresponding to particles of different sizes (1, 2.5, 4, and 10 micrometers), illustrate how each size behaves within the simulated environment over time. It is worth noting that smaller particles tend to remain airborne for longer periods due to their lower settling velocity. The data supports this notion, as the concentration levels of 1 μm particles consistently appear higher.

Finally, dust measurement inside the model was made using TSI particle sizer, the results can be seen in Fig. 14 d. In these 8 samples each sample for 20 s were made, the mean and stander division of them were made. The results show the size range of injected particle between 1 to 15 μm. The experimental setup offers a great opportunity to measure the dust concentration inside the model and outside it (the test section).

These results hold significant value because they showcase the system's ability to replicate real-world scenarios within a controlled environment. The capacity to manipulate the pump flow rate and observe the corresponding changes in airspeed and dust concentration is particularly relevant when it comes to evaluating the risks associated with inhalation of particles of different sizes under varying exertion conditions.

In recent advancements, the dust wind tunnel has broadened its scope to test and optimize a suite of dust mitigation technologies and protective measures. This includes a water spray system specifically designed to reduce dust concentrations—a crucial initiative for enhancing safety in coal mining environments. Fig. 15 provides a visual overview of the experimental setup within the wind tunnel, where this system, among others, is rigorously evaluated. The effectiveness of the water spray system in capturing and settling respirable dust particles is meticulously assessed, yielding essential insights that inform the optimization of this method for practical, real-world applications.

Furthermore, the wind tunnel's capabilities are leveraged to test additional dust control technologies such as electrostatic precipitators [41] and air curtains [42] or flooded-bed dust scrubber with vibrating mesh [43,44]. These systems, designed to remove or deflect dust

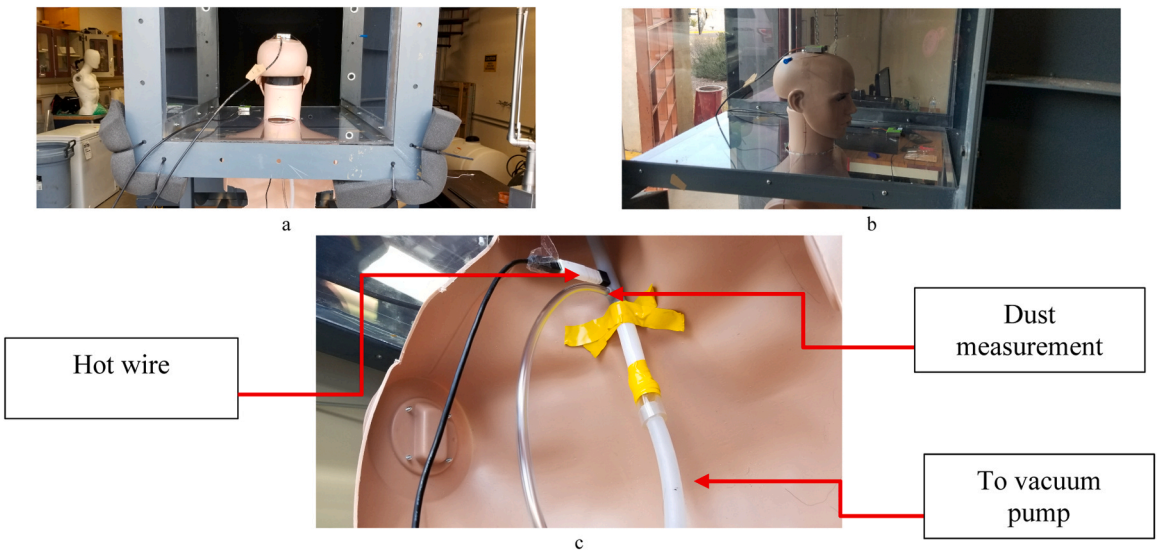

Fig. 13. Upper Respiratory Tract Simulation Model in Wind Tunnel. This experimental setup features a modified mannequin equipped with a throat-like structure connected to an aerosol particle sizer and vacuum pump to simulate inhalation, alongside a hot wire anemometer for measuring the velocity profile of inhaled air, facilitating detailed studies of aerosol inhalation dynamics.

particles from work areas, can be fine-tuned within the controlled environment of the wind tunnel to evaluate their effectiveness under various operational conditions. This allows for the development of highly effective, customized solutions tailored to the specific needs of mining operations.

This research further investigates the efficacy of various types of face masks and respirators under simulated conditions. This evaluation involves testing existing models and prototyping new designs with advanced filtration materials and ergonomic features for improved fit and comfort, as demonstrated in Fig. 15. Here, the effectiveness of face masks and shields is assessed in the dust wind tunnel. A specific focus is on the concentration entrained in ALDA compared to the dust concentration in the wind tunnel (concentration ratio %), showing that the face shield reduces the dust concentration entering ALDA by 69.4 %. The ultimate goal is to equip miners with masks that provide optimal protection against fine dust, enhance comfort, and improve usability, thereby reducing wear-related issues [45].

Additionally, the wind tunnel is used to simulate the effectiveness of real-time dust monitoring systems, which can trigger automatic activation of dust suppression technologies based on detected dust levels. This integration of responsive control systems represents a significant step forward in proactive dust management. The dust wind tunnel can be used in different applications as well and it is not primarily for coal dust; for example, it could be used to evaluate the effectiveness of various biogenic materials in suppressing wind-induced dust emissions in mining environments [46].

By utilizing the dust wind tunnel, we can conduct comprehensive, precise testing of these innovative solutions. Each aspect of this study supports the advancement of dust suppression technologies and enhances our understanding of protective gear performance, directly impacting health and safety protocols in mining operations. Through these investigations, the wind tunnel proves to be an indispensable tool for advancing occupational health and safety, enabling precise testing and development of dust management strategies and protective equipment.

7. Conclusion

The research presented herein has systematically addressed the challenge of simulating the aerodynamic conditions prevalent in underground coal mines, with a focus on the associated dust dispersion and its potential impact on workers' health. The methodology encompassed a comprehensive approach that included the design, optimization, and validation of a specialized wind tunnel tailored for this purpose. The optimization of the wind tunnel design was conducted through the integration of computational fluid dynamics (CFD) and response surface methodology, ensuring that the simulated conditions were refined to closely replicate those of an underground coal mine environment. Empirical studies conducted within the wind tunnel provided a wealth of data on dust behavior, facilitated by a bespoke dust injection system and the utilization of hot-wire anemometry for precise airflow measurement. The incorporation of a respiratory tract model, equipped to simulate inhalation through a vacuum pump and to measure dust concentrations via an aerosol particle sizer, was instrumental in elucidating the interaction between inhaled particulates and human respiratory function. Adjustments to the pump flow rate mirrored various breathing intensities, allowing for a nuanced exploration of how changes in airflow affect dust concentration and distribution within the respiratory tract model. These experiments yielded critical insights into the dynamics of dust inhalation and the factors that influence exposure levels. The implications of this research for occupational health are substantial. By providing a quantitative assessment of dust exposure risks under varied aerodynamic conditions, the study contributes valuable knowledge to the domain of mine safety and worker protection.

Laboratory-generated dust exhibited characteristics akin to those of mine-generated dust, with predominantly irregular particle sizes ranging from 1.55 to 3.8 μm. Over 60 % of these particles were classified as PM4, categorizing them within the respirable range. Additionally, laboratory analyses detected titanium in coal samples at concentrations of 1.5 % to 3 % in the form of TiO2, further validating that the laboratory conditions effectively replicate the physical attributes observed in mining environments.

The wind tunnel operated at airflow speeds between 0.5 m/s and 3.0 m/s, successfully maintaining a uniform flow with turbulence levels consistently below 10 %. This setup was designed to mirror the actual aerodynamic conditions prevalent in underground mines, ensuring the relevance and applicability of the simulation results.

Quantitative analysis from the dust experiments illustrated the impact of adjusting the dust generator settings on spatial dust distribution within the tunnel. Notably, increasing the output from 10 g/min to 50 g/min caused a significant escalation in dust concentration, with peak values reaching up to 200 mg/m^3 in certain scenarios.

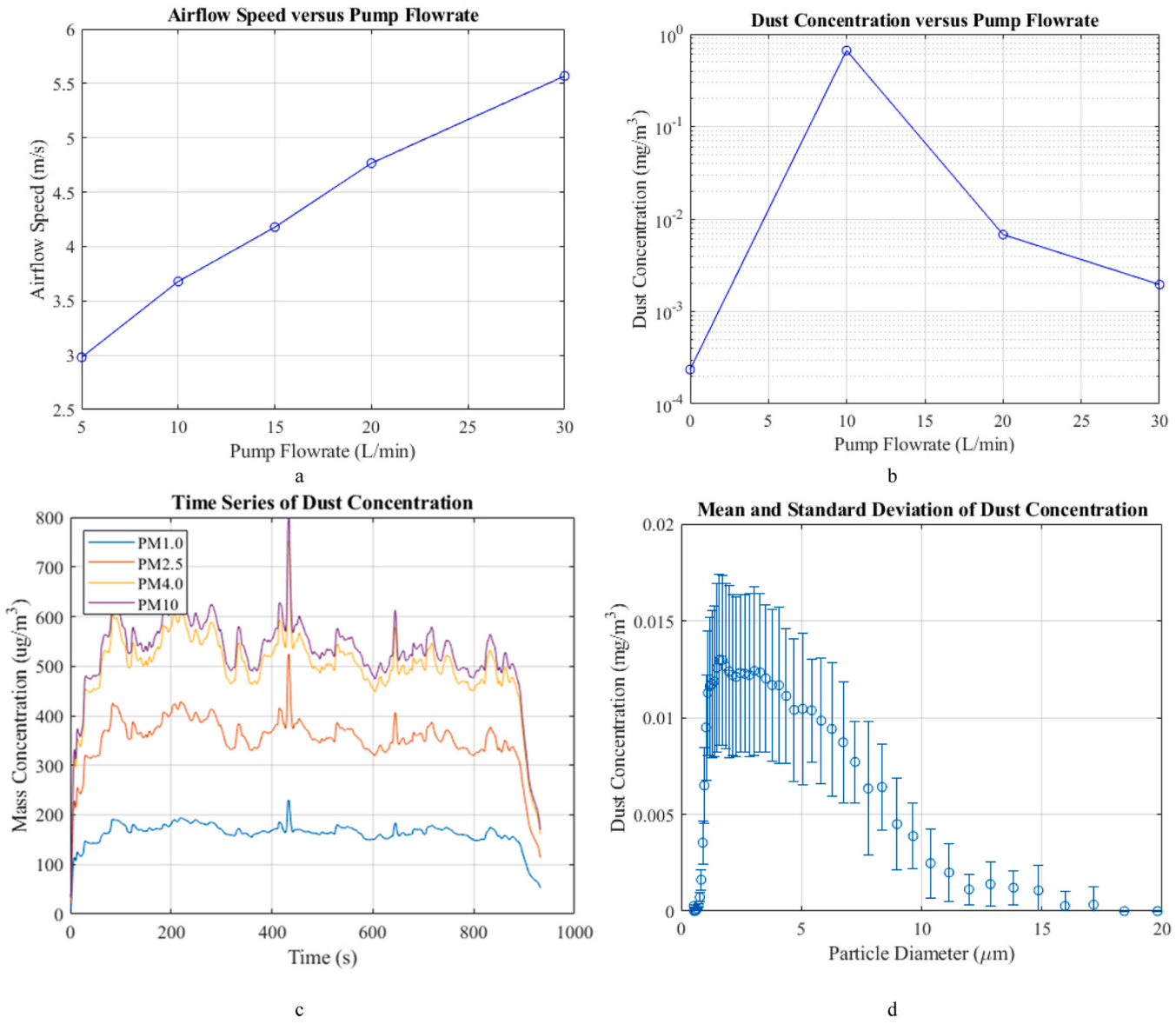

Fig. 14. The ALDA experiment results include: (a) a correlation of pump flow rate with airspeed, (b) the dust concentration entering ALDA at various pump flow rates, (c) a time history of dust concentration for different particle sizes in the wind tunnel, and (d) the particle size distribution entering ALDA.

In the face shield experiments, there was a marked reduction in dust penetration into the ALDA, with a decrease of approximately 70 % in dust entry. This result underscores the effectiveness of protective measures in mitigating respirable dust exposure.

To further validate the findings from this study and enhance the practical application of the technologies developed, it is essential to extend our research beyond simulated environments. Future studies should focus on field validation in actual underground coal mine settings. This step will allow us to test the effectiveness of the dust management strategies and protective equipment in real-world conditions, ensuring that the dust wind tunnel is both practical and effective in enhancing miner safety. Such field tests will provide critical feedback for refining our wind tunnel simulations and contribute to more robust occupational health practices. Continued research into the mechanisms of dust and water droplet injection in wind tunnels is essential for advancing our capabilities in environmental control within such settings. Future investigations will focus on refining the injection techniques to achieve more uniform distribution and enhanced interaction between dust particles and water droplets. These efforts are expected to significantly improve the design and efficiency of wind tunnels, contributing to more effective dust suppression technologies and practices that can be applied not only in laboratory settings but also in industrial applications where air quality control is critical.

Environmental Implication

The design and validation of this wind tunnel have significant environmental implications, particularly in enhancing occupational health and safety in coal mining. By accurately simulating real-world conditions, this research allows for the precise assessment and mitigation of respirable dust hazards. The findings can inform the development of more effective dust control strategies and protective equipment, ultimately reducing the health risks faced by miners and contributing to cleaner, safer mining operations. Additionally, this research supports regulatory efforts to improve air quality standards in industrial environments, promoting broader public health benefits.

CRediT authorship contribution statement

Ahmed Aboelezz: Writing – original draft, Visualization, Validation,

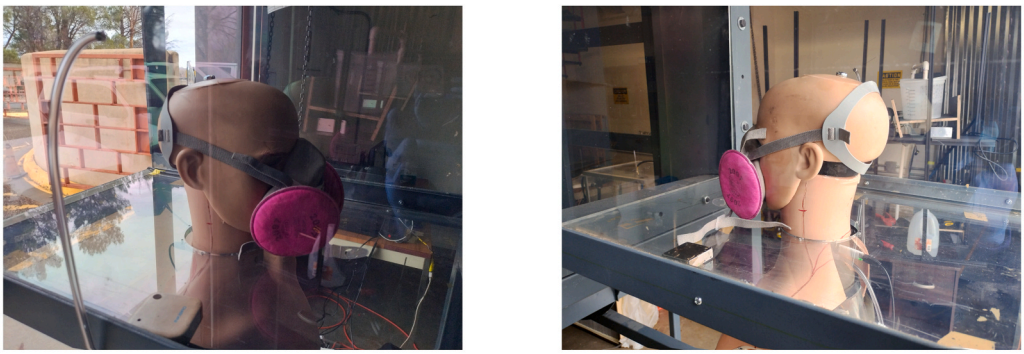

Face mask during the testing

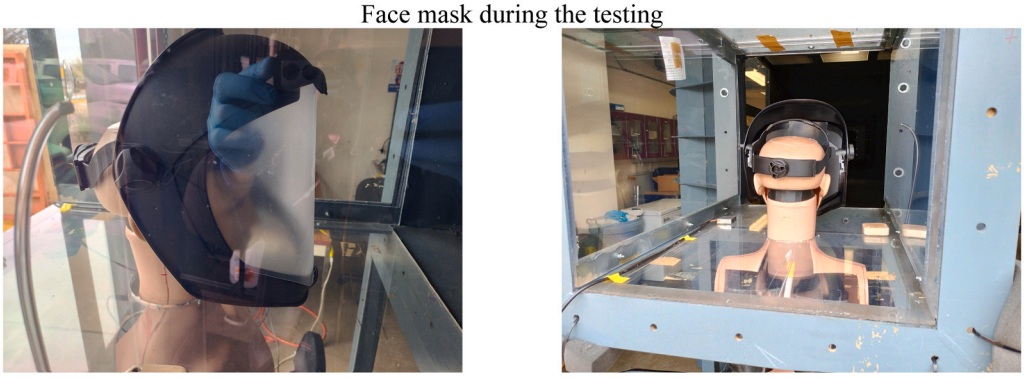

Face shield dusring the testing

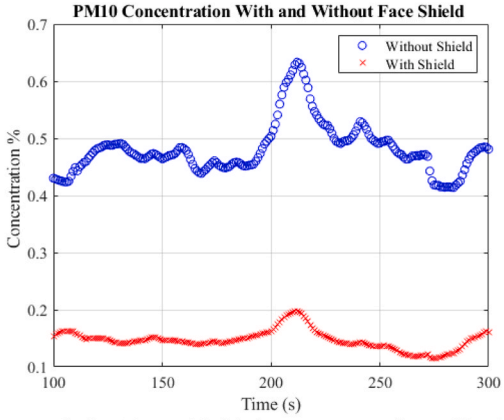

Sample result for Face shield dust preventation effectifness

Water spray off Water spray on

Water spray testing

Fig. 15. This figure illustrates testing framework where a water spray system is evaluated for its efficacy in dust suppression alongside various face masks. The tests aim to determine optimal conditions for reducing respirable dust concentrations, thereby enhancing miner safety in coal mining environments.

Software, Methodology, Investigation, Formal analysis, Data curation, Conceptualization. **Michael Hargather:** Writing – review & editing, Writing – original draft, Validation, Resources, Investigation. **Maria Beltran:** Writing – original draft, Investigation, Formal analysis, Data curation, Conceptualization. **Pedram Roghanchi:** Writing – review & editing, Writing – original draft, Validation, Supervision, Software, Resources, Project administration, Funding acquisition, Conceptualization. **Mostafa Hassanalian:** Writing – review & editing, Writing – original draft, Validation, Supervision, Software, Resources, Methodology, Investigation, Conceptualization.

Declaration of Competing Interest

The authors declare that they have no known competing financial interests or personal relationships that could have appeared to influence the work reported in this paper.

Data Availability

No data was used for the research described in the article.

Acknowledgements

This research was funded by National Institute for Occupational Safety and Health (NIOSH), grant numbers #75D30119C06390 and #75D30121C12182. The views, opinions, and recommendations expressed here are solely those of the authors and do not necessarily reflect the views of NIOSH. Mention of trade names, commercial products, or organizations does not imply endorsement by the authors or the funding organization. The authors thank Maria Pineda, and Carlha Barreto for helping with the sample preparation, and Virgil Lueth, Bonnie Frey, and Kelsey McNamara at the New Mexico Bureau of Geology for providing training to perform XRD and total microwave digestion experiments.

References

[1] Bodenhamer, A.A. (2020). Outlaw Operators: Prevention Failures and the Resurgence of Black Lung in Central Appalachia. Carsey Research, National Issue Brief #149, Summer 2020. University of New Hampshire, Carsey School of Public Policy.
[2] Liu, T., Liu, S., 2020. The impacts of coal dust on miners' health: a review. Environ Res vol. 190 (May), 109849. https://doi.org/10.1016/j.envres.2020.109849.
[3] Han, S., Chen, H., Harvey, M.-A., Stemn, E., Cliff, D., 2018. Focusing on coal workers' lung diseases: a comparative analysis of China, Australia, and the United States. Int J Environ Res Public Health. https://doi.org/10.3390/ijerph15112565.
[4] Shekarian, Y., Rahimi, E., Rezaee, M., Su, W.C., Roghanchi, P., 2021. Respirable coal mine dust: a review of respiratory deposition, regulations and characterization. Minerals vol. 11 (7), 1–25. https://doi.org/10.3390/min11070696.
[5] Abbasi, B., et al., 2021. Review of respirable coal mine dust characterization for mass concentration, size distribution and chemical composition. Mineral Charact Occup Environ Dust Expo vol. 11 (426). https://doi.org/10.3390/min11040426.
[6] Perret, J.L., et al., 2017. Coal mine dust lung disease in the modern era. Respirology vol. 22 (4), 662–670. https://doi.org/10.1111/resp.13034.
[7] Azam, S., Mishra, D.P., 2019. Effects of particle size, dust concentration and dust-dispersion-air pressure on rock dust inertant requirement for coal dust explosion suppression in underground coal mines. Process Saf Environ Prot vol. 126, 35–43. https://doi.org/10.1016/j.psep.2019.03.030.
[8] Cao, W., Huang, L., Zhang, J., Xu, S., Qiu, S., Pan, F., 2012. Research on characteristic parameters of coal-dust explosion. Procedia Eng vol. 45, 442–447. https://doi.org/10.1016/j.proeng.2012.08.183.
[9] Zhou, Q., Qin, B., Oct. 2021. Coal dust suppression based on water mediums: a review of technologies and influencing factors. Fuel vol. 302, 121196. https://doi.org/10.1016/J.FUEL.2021.121196.
[10] Bałaga, Dominik, Siegmund, Michał., Kalita, Marek, Williamson, Ben J., Walentek, Andrzej, Małachowski, Marcin, 2021. Selection of operational parameters for a smart spraying system to control airborne PM10 and PM2. 5 dusts in underground coal mines. Process Saf Environ Prot 148, 482–494.
[11] Zheng, Haotian, Jiang, Bingyou, Zheng, Yuannan, Zhao, Yang, Wang, Haoyu, 2023. Experimental study on forced ventilation and dust-control in a heading face based on response surface method. Process Saf Environ Prot 175, 753–763.
[12] Nie, Wen, Zhang, Yilong, Guo, Lidian, Zhang, Xu, Peng, Huitian, Chen, Dawei, 2023. Research on airborne air curtain dust control technology and air volume optimization. Process Saf Environ Prot 172, 113–123.
[13] Cao, Yong, Xiao, Yang, Wang, Zhen-Ping, Li, Qing-Wei, Shu, Chi-Min, Jiang, Xing-Rui, Wu, Shi-Liang, 2024. Recent progress and perspectives on coal dust sources, transport, hazards, and controls in underground mines. Process Saf Environ Prot.
[14] Sieger, Johannes L., Bernd, G.Lottermoser, Freer, Justus, 2023. Effectiveness of protein and polysaccharide biopolymers as dust suppressants on mine soils: results from wind tunnel and penetrometer testing. Appl Sci 13 (7), 4158.
[15] Wu, Hao, Liu, Meng, Mi, Youzhi, Wang, Jun, Guo, Menglei, 2022. Key parameters of a design for a novel reflux subsonic low-density dust wind tunnel. Aerospace 9 (11), 662.
[16] Esders, Eike Maximilian, Sittl, Sebastian, Krammel, Inka, Babel, Wolfgang, Papastavrou, Georg, Thomas, Christoph Karl, 2023. Is transport of microplastics different from that of mineral dust? Results from idealized wind tunnel studies. EGUsphere 2023, 1–26.
[17] Richards-Thomas, T., Neuman, C.M.K., 2023. Wind tunnel experiments on volcaniclastic dust emission and dispersion initiated by water droplet impact. J Geophys Res: Atmospheres 128 no. 11 e2022JD038149.
[18] Ji, Wenjing, Zhao, Bin, 2018. A wind tunnel study on the effect of trees on PM2. 5 distribution around buildings. J Hazard Mater 346, 36–41.
[19] Barlow, J.B., Rae, W.H., & Pope, A. "Low-speed wind tunnel testing," John Wiley & Sons, 1999.
[20] Taylor, C.D., R.J. Timko, M.J. Senk, and A. Lusin. "Measurement of airflow in a simulated underground mine environment using an ultrasonic anemometer." (2003).
[21] Mehta, R.D., 1979. The aerodynamic design of blower tunnels with wide-angle diffusers. Prog Aerosp Sci Vol. 18, 59–120.
[22] Prostański, D., 2013. Use of air-and-water spraying systems for improving dust control in mines. J Sustain Min vol. 12 (2), 29–34. https://doi.org/10.7424/jsm130204.
[23] D. Prostański, "Dust control with use of air-water spraying system," Arch. Min. Sci., vol. 57, no. 4, pp. 975–990, Dec. 2012, doi: 10.2478/V10267–012-0065–7.
[24] Zhang, Q., et al., 2022. A review of physical and chemical methods to improve the performance of water for dust reduction. Process Saf Environ Prot vol. 166 (July), 86–98. https://doi.org/10.1016/j.psep.2022.07.065.
[25] Pereira, J.D., 2011. Wind Tunnels: Aerodynamics, Models and Experiments. Nova Science Publishers,.
[26] Aboelezz, A., 2019. Low speed wind tunnel design and optimization using computational techniques and experimental validation. Incas Bull Vol. 11 (No. 2), 3–13.
[27] Salinas, V., et al., 2022. Characterization and toxicity analysis of lab-created respirable coal mine dust from the appalachians and rocky mountains regions. Minerals vol. 12 (7), 1–29. https://doi.org/10.3390/min12070898.
[28] Gupta, R., 2007. Advanced coal characterization: a review. Energy Fuels vol. 21 (2), 451–460. https://doi.org/10.1021/ef060411m.
[29] Gaudette, H.E., 1964. The Nature of Illite. Clays Clay Min vol. 13 (1), 33–48. https://doi.org/10.1346/ccmn.1964.0130105.
[30] Hower, John, Thomas, C.Mowatt, 1966. The mineralogy of illites and mixed-layer illite/montmorillonites. Am Miner: J Earth Planet Mater 51 (5-6), 825–854.
[31] Velde, B., 1966. Upper stability of muscovite. Am Mineral vol. 51 (5–6), 924–929.
[32] Swanson, Vernon Emanuel, J.Hatch Medlin, J.R. Hatch, S.L. Coleman, G.H. Wood Jr, S.D. Woodruff, and R.T. Hildebrand. Collection, chemical analysis, and evaluation of coal samples in 1975. No. 76–468. US Geological Survey, 1976.
[33] Finkelman, Robert B. Modes of occurrence of trace elements in coal. No. 81–99. US Geological Survey, 1981.
[34] Hower, J.C., Eble, C.F., Wang, N., Dai, S., 2021. Distribution of rare earth elements and other critical elements in beneficiated Pennsylvania anthracites. Fuel 304. https://doi.org/10.1016/j.fuel.2021.121400.
[35] Racovita, A.D., 2022. Titanium dioxide: structure, impact, and toxicity. Int J Environ Res Public Health Vol. 19 (Issue 9). https://doi.org/10.3390/ijerph19095681.
[36] Vinu, A., Mori, T., Ariga, K., 2006. New families of mesoporous materials. Sci Technol Adv Mater vol. 7 (8), 753–771. https://doi.org/10.1016/j.stam.2006.10.007.
[37] Antonelli, David M., Jackie, Y.Ying, 1996. "Mesoporous materials. Curr Opin Colloid Interface Sci 1 (4), 523–529.
[38] Das, M., Salinas, V., LeBoeuf, J., Khan, R., Jacquez, Q., Camacho, A., Hovingh, M., Zychowski, K., Rezaee, M., Roghanchi, P., Rubasinghege, G., 2023. A toxicological study of the respirable coal mine dust: assessment of different dust sources within the same mine. Minerals 13 (3). https://doi.org/10.3390/min13030433.
[39] Sarver, E., Keles, C., Rezaee, M., 2019. Beyond conventional metrics: comprehensive characterization of respirable coal mine dust. Int J Coal Geol 207, 84–95. https://doi.org/10.1016/j.coal.2019.03.015.

[40] Su, Wei-Chung, Chen, Yi, Xi, Jinxiang, 2020. Estimation of the deposition of ultrafine 3D printing particles in human tracheobronchial airways. J Aerosol Sci 149, 105605.
[41] Popa, G., Diniș, C., & Iagăr, A. (2023). Investigations on Three-Section Plate-Type Electrostatic Precipitators Used in Thermoelectric Power Plants. Energies.
[42] Yan, X., Yang, H., Mo, H., Xie, Y., Jin, Z., & Zhou, Y. (2023). Numerical Simulation on the Smoke Prevention Performance of Air Curtains in an Island-Type Subway Station. Fire.
[43] Liao, L., Xiao, W., Zhao, M., Yu, X., Wang, H., Wang, Q., Chu, S., & Cui, Y. (2020). Can N95 Respirators Be Reused after Disinfection? How Many Times?. ACS Nano.
[44] Lu, Z. et al. (2022). A computational fluid dynamics investigation of a novel flooded-bed dust scrubber with vibrating mesh, https://doi.org/10.1016/j.ijmst.2022.03.002.
[45] Uluer, M.E. et al. (2023). An Exploratory Investigation on the Effectiveness of a Novel Vibration-Enhanced Flooded Bed Dust Scrubber, https://doi.org/10.1007/s42461–023-00889-w.
[46] Freer, Justus, et al., 2022. Effectiveness of food processing by-products in suppressing wind-induced dust emissions from mine soils: results from laboratory wind tunnel experiments. SSRN Electron J.